Arch. Metall. Mater. **66** (2021), 2, 489-495

DOI: 10.24425/amm.2021.135883

L. SOWA[1*], T. SKRZYPCZAK[1], P. KWIATOŃ[1]

INFLUENCE OF LIQUID METAL MOVEMENTS ON THE CASTING CREATION

Knowledge about complex physical phenomena used in the casting process simulation requires continuous complementary research and improvement in mathematical modeling. The basic mathematical model taking into account only thermal phenomena often becomes insufficient to analyze the process of metal solidification, therefore more complex models are formulated, which include coupled heat-flow phenomena, mechanical or shrinkage phenomena. However, such models significantly complicate and lengthen numerical simulations; therefore the work is limited only to the analysis of coupled thermal and flow phenomena. The mathematical description consists then of a system of Navier-Stokes differential equations, flow continuity and energy. The finite element method was used to numerically modeling this problem. In computer simulations, the impact of liquid metal movements on the alloy solidification process in the casting-riser system was assessed, which was the purpose of this work, and the locations of possible shrinkage defects were pointed out, trying to ensure the right supply conditions for the casting to be free from these defects.

Keywords: Numerical simulations, solidification, Navier-Stokes equations

1. Introduction

The production of high-quality castings requires technological improvement of the casting methods. All such operations are essentially aimed at obtaining high strength castings without casting defects. Conducting research on real objects is much more difficult due to the lack of visibility and high temperatures taking place there, therefore computer simulations are one of the frequently used methods of improving the casting process [1-12]. This requires the formulation of an appropriate mathematical model that takes into account the mutual influence of thermal and flow phenomena (complex model) [2,3,5,6]. Some researchers neglect the movements of liquid metal in the numerical analysis of the solidification process (basic model) [4,8], but, in turn, they focus on the analysis of the formation and growth of shrinkage defects in the casting process [4]. It is also possible to find works that deal with an in-depth analysis of phenomena occurring in the mushy zone on the basis of micro-macro modelling of the solidification process taking into account the movements of liquid metal in the interdendric space [12]. This article analyses the solidification process of a casting using both a complex and basic model with two variants of initial conditions only on a macroscopic scale. In this way, the influence of taking into account or ignoring the movements of the liquid metal on the process of making a casting without shrinkage defects was assessed, which was the main purpose of this work. The effectiveness of feeding the casting through the molten metal from the riser with the assumed dimensions and cylindrical shape was also checked. By observing the permanently changing shape of the solidus line, it was assessed whether it was closed in the area of the casting feed. Such a situation would mean no feeding of this area with liquid metal from the riser and the formation of shrinkage defects at this point of the casting. In order to verify the results obtained from numerical simulations, a test casting was made with the same geometrical, material and technological conditions as in the numerical simulations. Only in the case of the numerical results obtained from the models taking into account the movements of liquid metals in the filling process, was their good agreement with the results of the experiment. This is because the models taking into account the movements of the molten metal more accurately reflect the real conditions in the cavity of the casting mould during formation of the casting.

2. The mathematical model

The mathematical description of the casting solidification process considering the liquid metal movements is based on the

[1] CZESTOCHOWA UNIVERSITY OF TECHNOLOGY, DEPARTMENT OF MECHANICS AND MACHINE DESIGN FUNDAMENTALS, 73 DĄBROWSKIEGO STR., 42-200 CZĘSTOCHOWA, POLAND

* Corresponding author: sowa@imipkm.pcz.pl

solution of the following equations system (the Navier-Stokes equations (1), the continuity equation (2), the heat conductivity equation with the convection term (3), the first order pure advection equation (4)) in a cylindrical axial-symmetric coordinate system [2-6]:

$$\mu\left(\frac{\partial^2 v_r}{\partial r^2}+\frac{1}{r}\frac{\partial v_r}{\partial r}+\frac{\partial^2 v_r}{\partial z^2}-\frac{v_r}{r^2}\right)-\frac{\partial p}{\partial r}+$$
$$+\rho g_r+\rho g_r\beta\left(T-T_\infty\right)=\rho\frac{dv_r}{dt},$$
$$\mu\left(\frac{\partial^2 v_z}{\partial r^2}+\frac{1}{r}\frac{\partial v_z}{\partial r}+\frac{\partial^2 v_z}{\partial z^2}\right)-\frac{\partial p}{\partial z}+$$
$$+\rho g_z+\rho g_z\beta\left(T-T_\infty\right)=\rho\frac{dv_z}{dt} \quad (1)$$

$$\frac{\partial v_r}{\partial r}+\frac{v_r}{r}+\frac{\partial v_z}{\partial z}=0 \quad (2)$$

$$\frac{\lambda}{r}\frac{\partial T}{\partial r}+\frac{\partial}{\partial r}\left(\lambda\frac{\partial T}{\partial r}\right)+\frac{\partial}{\partial z}\left(\lambda\frac{\partial T}{\partial z}\right)=$$
$$=\rho C_{ef}\frac{\partial T}{\partial t}+\rho C_{ef}\left(v_r\frac{\partial T}{\partial r}+v_z\frac{\partial T}{\partial z}\right) \quad (3)$$

$$\frac{\partial F}{\partial t}+v_r\frac{\partial F}{\partial r}+v_z\frac{\partial F}{\partial z}=0 \quad (4)$$

where: $\lambda(T)$ – the thermal conductivity coefficient [W/(m·K)], $\mu(T)$ – the dynamic viscosity coefficient [kg/(m·s)], $\rho = \rho(T)$ – the density [kg/m^3], v_r, v_z – the r-component and z-component of velocity, respectively [m/s], T – the temperature [K], $C_{ef} = c_{LS}+L/(T_L - T_S)$ – the effective specific heat of a mushy zone [J/(kg·K)], L – the latent heat of solidification [J/kg], g_r, g_z – the r- and z-component of gravitational acceleration, respectively [m/s^2], p – the pressure [N/m^2], β – the volume coefficient of thermal expansion [1/K], t – the time [s], c_{LS} – the specific heat of a mushy zone [J/(kg·K)], r – the radius [m], T_∞ – the reference temperature ($T_\infty = T_{in}$) [K], F – the pseudo-concentration function across the elements lying on the free surface, α_M – the heat transfer coefficient between the ambient and the mould [W/(m^2·K)], T_a – the ambient temperature [K], T_L, T_S – the liquidus and solidus temperature of the analysed alloy [K], T_A – the temperature of air inside mould cavity in initial state [K], λ_M – the thermal conductivity coefficient of mould [W/(m·K)], v_t, v_n – the tangential and normal component of velocity vector, respectively [m/s], n – the outward unit normal surface vector.

The velocity and pressure fields were obtained from the solution of momentum equations (1) and continuity equation (2), while temperature field from solving the equation of heat conductivity with the convection term (3). The predicting the filling behaviours of molten metal and the free surface (air-fluid interface) movement is described by the first order pure advection equation (4). The pseudo-concentration function F, which is obtained from the solution of equation (4), is a continuous function varying from 0 to 1 on the elements lying on the free surface and can be considered as a fictitious property of the fluid. We can assign the value 1 to regions where fluid has already entered and the value of 0 to air-filled regions. The position of the fluid front (the free surface) is determined by the iso-value contour $\in$ [0; 1] (cells cut by the interface) in any control volume that moves with the free velocity field. The mathematical description of the solidification process of the casting without taking into account the movements of liquid metal is reduced only to the solution of the heat conductivity equation (3) without the convection term [4,8].

The system of equations (1-4) was supplemented with appropriate initial conditions [5] and boundary conditions, which were assumed on the indicated surfaces (Fig. 1) [3-5]. This task was solved using the FEM in the weighted residuals formulation [3-5].

3. Description of the problem

To analyse the impact of the movements of the liquid metals alloy on solidification of the casting, the following casting-riser-mould system was considered (Fig. 1).

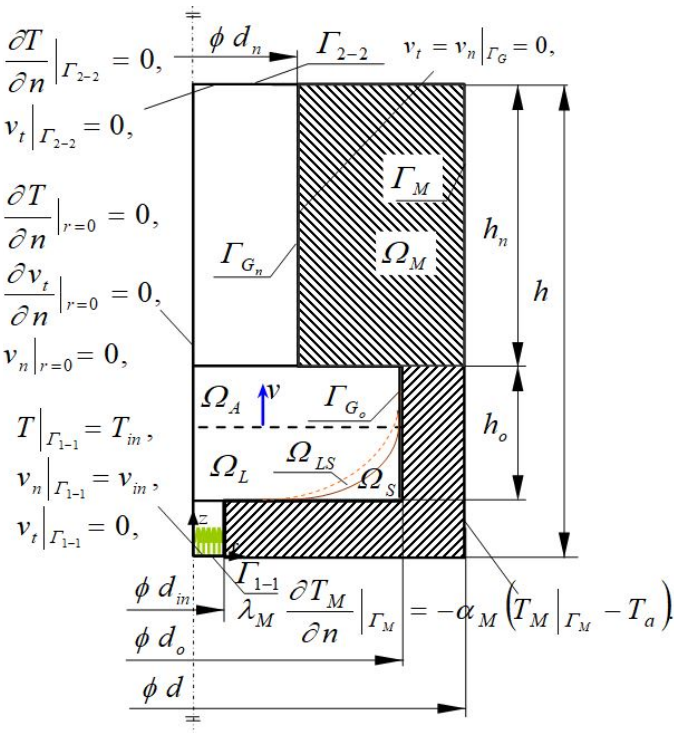

Fig. 1. Boundary conditions, scheme and identification of sub-regions of the considered region

The outside mould dimensions are equal to: d = 0.320 m, h = 0.280 m, whereas the mould cavity dimensions are equal to: d_o = 0.200 m, h_o = 0.070 m, h_n = 0.150 m, d_n = 0.080 m, d_{in} = 0.020 m. The internal surface of the steel mould is covered with a protective coating with 2 mm thickness. The numerical simulations were carried out for the casting made of low-carbon

cast steel and the steel mould. The thermo-physical properties were taken from work [5] and are summarised in Table 1 for casting and Table 2 for other regions under consideration. The overheated metal with temperature T_{in} = 1835 K has been poured from the bottom with the velocity v_{in} = 0.1 m/s, into the steel mould with initial temperature T_M = 350 K. Other important temperatures were equal to: T_A = 350 K, T_a = 300 K. The heat transfer coefficient (α) between ambient and the mould was equal to α_M = 200 W/(m^{2}K).

TABLE 1

Material properties of the casting – cast steel

Material property	**Solid phase ($T_M - T_S$)**	**Liquid phase ($T_L - T_{in}$)**
ρ [kg/m^3]	7805 – 7800	7300 – 7295
c [J/(kg·K)]	640 – 644	830 – 834
λ [W/(m·K)]	48 – 45	23 – 21
μ [kg/(m·s)]	10100 – 10000	0.006 – 0.0004
β [1/K]	0.000035	0.00014
Additional parameters		
T_L [K]	1810	
T_S [K]	1760	
L [J/kg]	270000	

TABLE 2

Material properties used in the calculations for other regions

Material property	**Mould**	**Protective coating**	**Air**
ρ [kg/m^3]	7700	1600	1.23
c [J/(kg·K)]	600	1670	1006
λ [W/(m·K)]	52	0.3	0.024
μ [kg/(m·s)]	—	—	0.000018

The professional Fidap program was used for the calculations. The geometry of system was divided into 4979 quadrilateral element. In order to validate the correctness of the obtained results from numerical simulations, the real test casting was made with the same conditions as in computer calculations. Confirmation of the correctness of the obtained results from numerical simulations carried out with the use of the complex model was obtained.

4. Results and discussion

The phenomena of heat transport and fluid flow occurring in the cavity of the casting mould were modelled in the study. By performing numerical simulations, the influence of the solidification modelling methods on the obtained results from numerical calculations was analysed, with the aim of obtaining a casting without shrinkage defects. Numerical calculations were performed for three variants of the solidification process: taking into account (complex model) or omitting the movements of the molten metal (basic model) and the mixed model being a combination of the two previous models.

In variant I, the numerical analysis was performed including the process of filling the mould cavity with molten metal and convection movements after its completion until the casting completely solidified (Figs 2-5). In variant II, the movements of the molten metal were neglected (Figs 6-8). As an initialling condition for the calculation of the solidification process, it was assumed that the mould cavity was completely filled with the molten metal at the pouring temperature (Fig. 6). In variant III, the movements of the molten metal were neglected (Figs 9-11). As an initialling condition for the calculations of the solidification process, it was assumed that the mould cavity was completely filled with molten metal with the temperature calculated in variant I, as in Fig. 3.

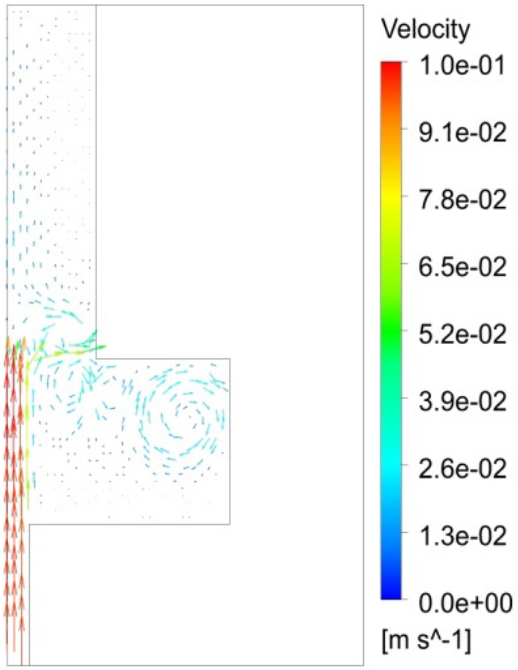

Fig. 2. Velocity vectors at t = 73 s, I variant

The simulations of the casting formation were made, starting from the moment of filling the mould cavity with molten metal and ending with its complete solidification. Filling the mould with liquid metal is shown in the form of velocity vectors for selected moment of time (Fig. 2 and 3). We can see here the main flow of molten metal only along the axis of symmetry of the casting and its slight movements in the rest of the casting. Figure 3 shows the temperature distribution corresponding to the velocity field at the final moment of filling the mould cavity, which is also the initial condition for the calculation of the solidification process in variant III. Observing here the solidus line on the temperature distribution, one can see solidification of the casting only in its lower corner, during this period of its creation. There is thus still liquid metal in the remainder of the mould cavity. Whereas, after mould filling, the velocity vectors and temperature distribution are shown in Figure 4, in which a solidus line was drawn separating the solid-liquid area of the casting from its solid area. During this solidification time, only very small movements of the liquid metal in the mushy zone

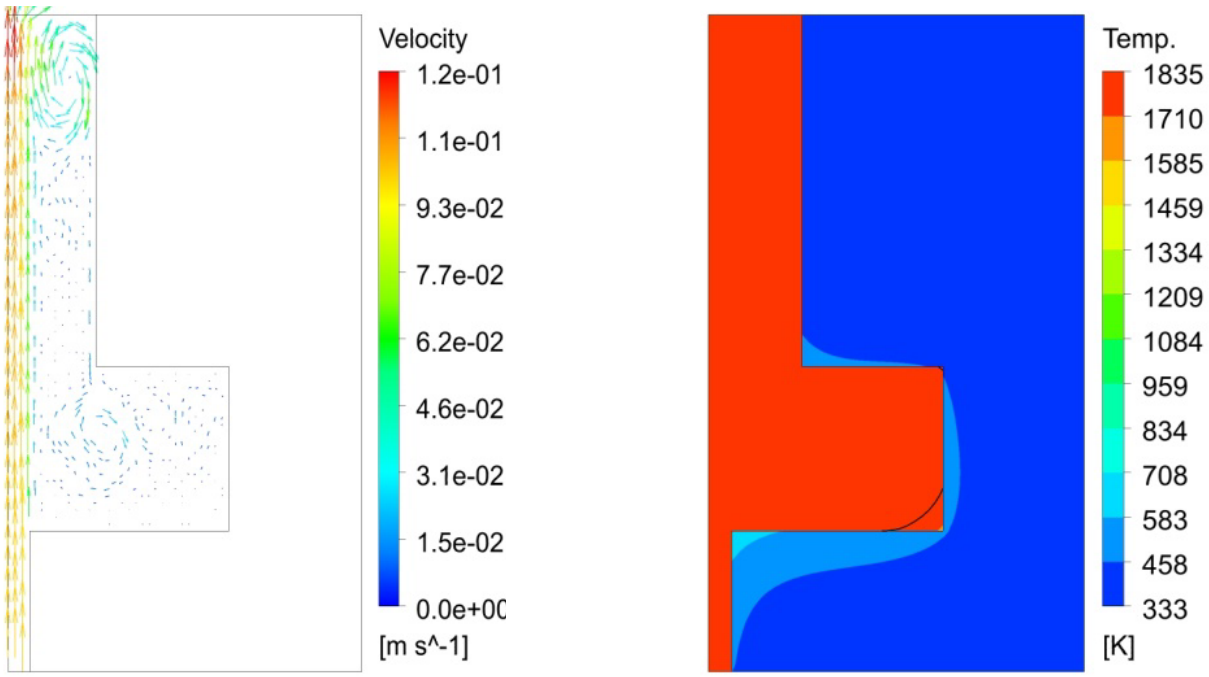

Fig. 3. Velocity and temperature fields at t = 100 s, I variant

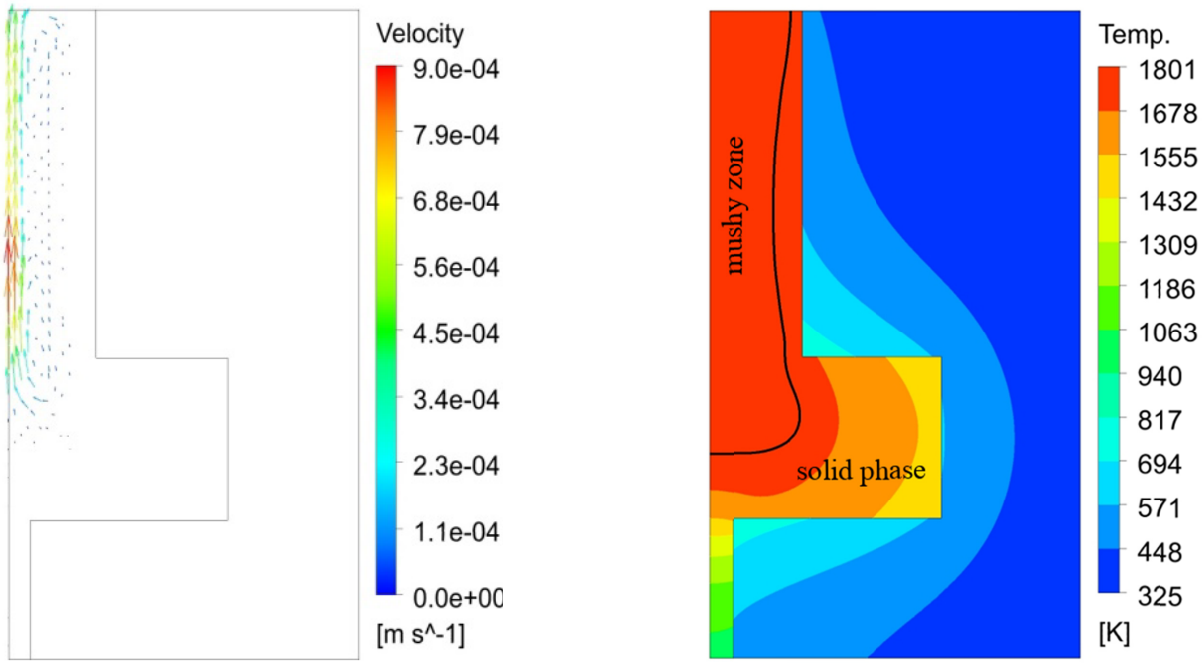

Fig. 4. Velocity and temperature fields at t = 400 s, I variant

are visible, because the forced metal flow disappears and only natural convection movements can be observed.

Then, the shape of the solidus line is observed in the final stages of solidification of the casting-riser system. After the solidus line is closed in the casting, the area delimited by it will not be supplied with the liquid metal from the riser, and a shrinkage defect will occur at this point as a result of metal shrinkage. Such a situation was not observed after solidification of the casting in the case of variant I and III (Fig. 5 and 11). In this figures, we can see that the solidus line is only in the riser which suggests that the casting remains free from shrinkage defects. Such state of the casting is confirmed by photos taken of the real test casting (Fig. 12).

Next, numerical simulations of the solidification process were performed using the basic and mixed models (variant II and III), in which the movements of the liquid metal were not taken into account. The obtained results of these calculations, in the form of temperature fields, for selected time steps are shown in Figs 6-8 (variant II) and Figs 9-11 (variant III). Observing the shape and position of the solidus line, it can be seen that the

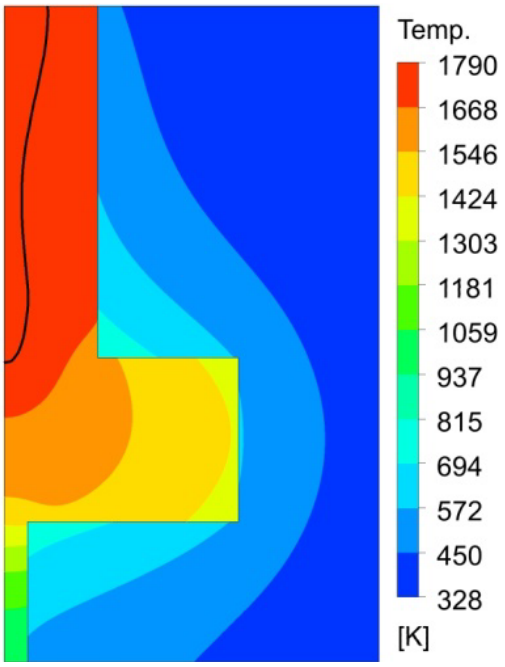

Fig. 5. Temperature distribution after solidification of the casting: t = 512 s, I variant

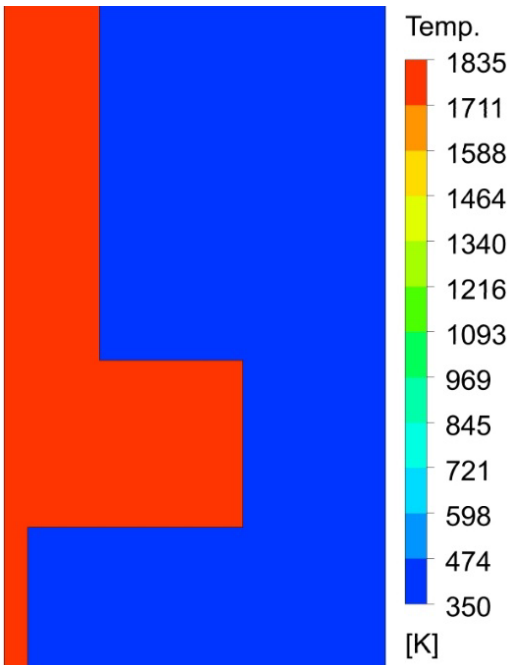

Fig. 6. Temperature field at t = 0 s, initial condition for II variant

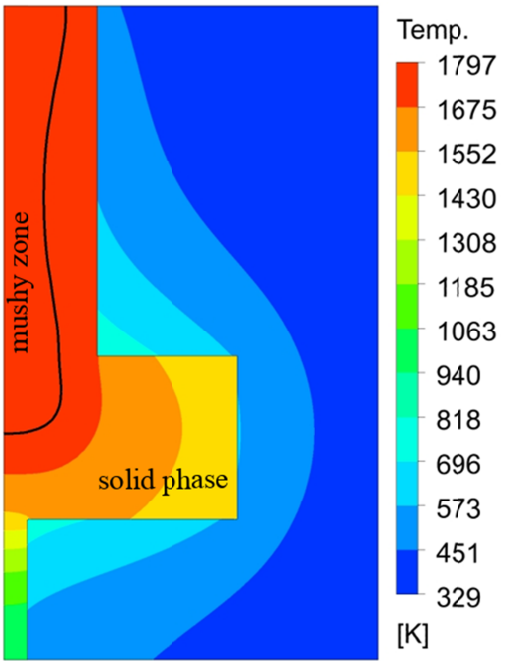

Fig. 7. Temperature field at t = 400 s, II variant

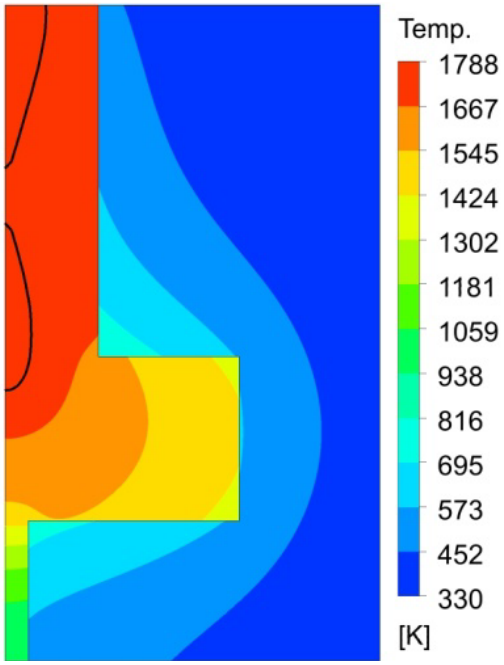

Fig. 8. Temperature distribution after solidification of the casting: t = 450 s, II variant

solidus line did not leave the upper part of the casting (Fig. 8), which may suggest the formation of a shrinkage defect in this place. Such a situation was not observed after solidification of the casting in the case of variant III (Fig. 11). The picture of the real test casting (Fig. 12) is presented in the form of a cross-section and a top view (after cutting off the riser and mechanical working the upper surface of the casting). The photo of the casting cross-section shows only slight defects in shape. However, there are no internal defects – the shrinkage cavities.

4. Conclusions

The article presents a mathematical model and the numerical simulations results of casting solidification, taking into account the process of filling the mould cavity with liquid metal and convection movements after its completion. The influence of molten metal movements on the solidification kinetics and the position of the solidification end in the considered system were assessed. Therefore, numerical calculations were performed

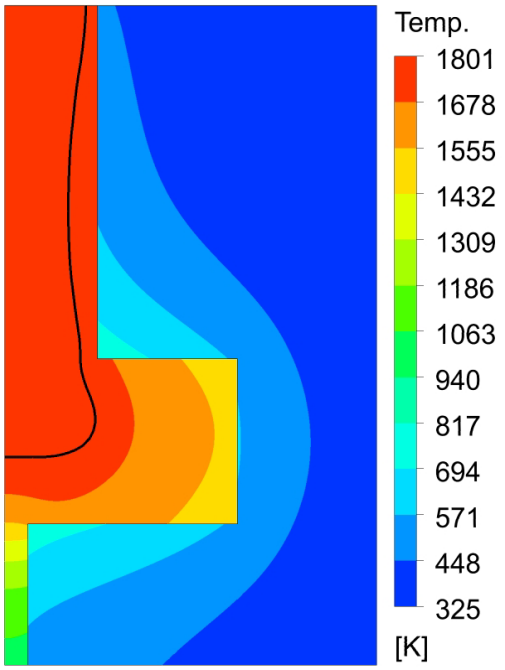

Fig. 9. Temperature fields at t = 300 s, III variant

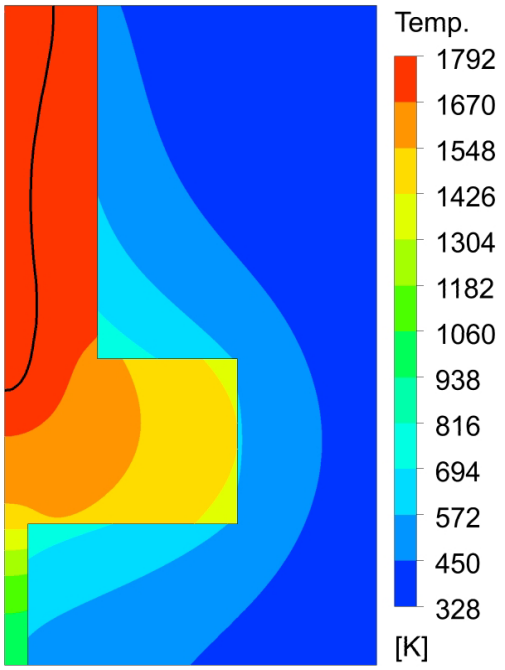

Fig. 10. Temperature fields at t = 400 s, III variant

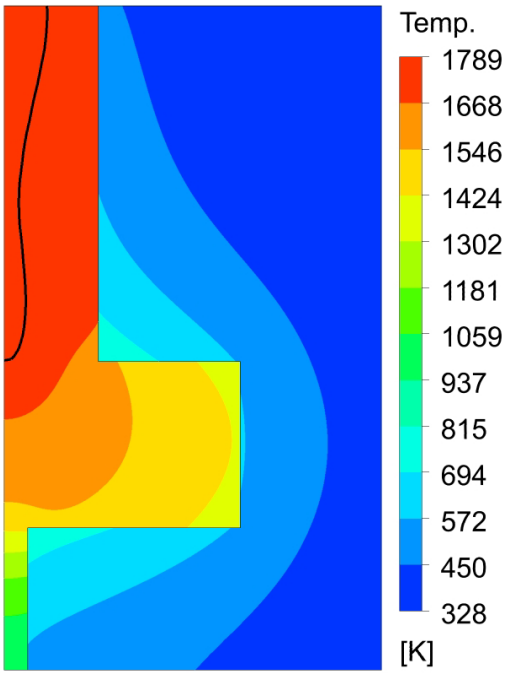

Fig. 11. Temperature distribution after solidification of the casting: t = 412 s, III variant

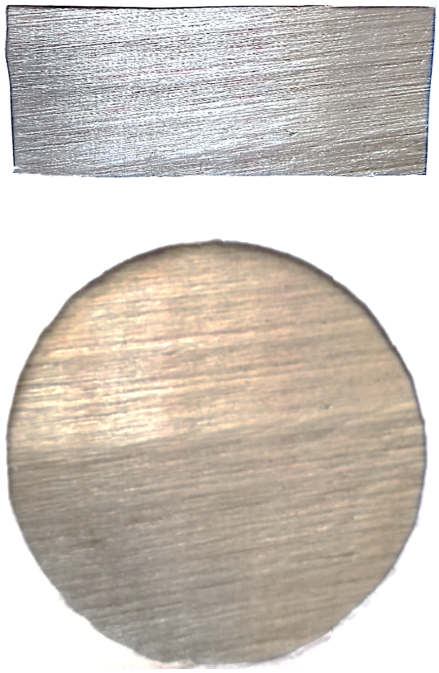

Fig. 12. Photo of the real test casting (cross section and top view)

for three variants of modelling the casting solidification process – with or without molten metal movements, using various initial conditions for temperature. The velocity and temperature fields obtained in this way make it possible to track the solidus line position in the subsequent stages of the calculations (Figs 3-11). It has been observed that the solidification process starts effectively for this casting shape when the mould cavity is completely filled with molten metal. In the final solidification period of the casting-riser system, the closure of the solidus line was observed and a possible localization of the shrinkage defect in the upper part of the casting, if the solidification process was carried out without taking into account the movements of the liquid metal (Fig. 8). The formation of the empty space cut off from the supply on the cast-riser interface does not necessarily mean that a shrinkage cavity in the upper part of the casting will form, because thanks to the filtration movements of the liquid phase in the interdendritic space, the lower part of the empty space can be filled, and a shrinkage cavity will only form in

the riser, as proved in [12]. Such a situation was not observed if the liquid phase movements were taken into account in the modelling of the casting solidification process (Fig. 5). In this case, the end of the solidification has taken place at the riser, which is desirable because the riser is cut off and reprocessed. A similar situation is in the case of variant III (Fig. 11), in which the calculations were carried out without taking into account the movements of the liquid metal but the temperature field from variant I at the time of complete filling of the mould cavity was adopted as the initial condition for calculations. You can see the complete similarity of the temperature distributions (variants I and III) in the time steps shown, resulting from the low value of the velocity of natural convection movements after filling the mould cavity in variant I. On the other hand, the movements of forced convection in the process of filling the mould cavity turn out to be important, as they carry the heat to the riser and therefore the end of solidification takes place there. It also proves that the cylindrical-shaped riser executed its task and the casting was made without shrinkage defects. Such state of the casting is confirmed by photos of the real test casting (Fig. 12). Thus, by considering the filling process and the convection movements of the molten metal in numerical analysis, the pouring conditions can be more accurately assessed and the location of the shrinkage cavity more precisely determined. Further research will be focused on assessing the impact of the riser shape and minimizing its dimensions on obtaining a casting without shrinkage defects, which is important for the foundry industry in economic terms.

REFERENCES

[1] S.L. Nimbulkar, R.S. Dalu, Perspectives in Science **8**, 39-42 (2016). DOI: 10.1016/j.pisc.2016. 03.001

[2] P.H. Huang, C.J. Lin, Int. J. Adv. Manuf. Technol. **79** (7), 997-1006 (2015). DOI: 10.1007/s00170-015-6897-5

[3] R.W. Lewis, E.W. Postek, Z. Han, D.T. Gethin, International Journal of Numerical Methods for Heat & Fluid Flow **16** (5), 539-572 (2006). DOI: 10.1108/09615530610669102

[4] T. Skrzypczak, L. Sowa, E. Węgrzyn-Skrzypczak, Archives of Foundry Engineering **20**(1), 37-42 (2020). DOI: 10.24425/afe.2020.131280

[5] L. Sowa, T. Skrzypczak, P. Kwiatoń, Archives of Foundry Engineering **20** (2), 31-36 (2020). DOI: 10.24425/afe.2020.131298

[6] P.H. Huang, J.K. Kuo, T.H. Fang, W. Wu, MATEC Web of Conferences. **185**, (2018). DOI: 10.1051/matecconf/ 201818500008

[7] D. Bartocha, T. Wróbel, J. Szajnar, W. Adamczyk, W. Jamrozik, M. Dojka, Arch. Metall. Mater. **62** (3), 1609-1613 (2017). DOI: 10.1515/amm-2017-0246

[8] A.S. Jabur, F.M. Kushnaw, J. Appl. Computat. Math. **6** (4), (2017). DOI: 10.4172/21689679.1000371

[9] A.A. Burbelko, D. Gurgul, M. Królikowski, M. Wróbel, Archives of Foundry Engineering **13** (4), 9-14 (2013). DOI:10.2478/afe-2013-0074

[10] J. Jezierski, R. Dojka, K. Janerka, Metals **8** (2018). DOI: doi.org/10.3390/met8040266

[11] M. Nadolski, A. Zyska, Z. Konopka, M. Łągiewka, J. Karolczyk, Archives of Foundry Engineering **11** (3), 141-144 (2011).

[12] R. Nadella, D.G. Eskin, Q. Du, L. Katgerman, Progress in Materials Science **53** (3), 421-480 (2008). DOI: doi.org/10.1016/j.pmatsci.2007.10.001